HOSTED BY
ELSEVIER
CrossMark
Available online at www.sciencedirect.com
ScienceDirect
Soils and Foundations 57 (2017) 645–654
SOILS AND FOUNDATIONS
www.elsevier.com/locate/sandf

Long-term strength of soil-cement columns in coastal areas

Pham Van Ngoc [a,b,*], Brett Turner [a], Jinsong Huang [a], Richard Kelly [c]

[a] Faculty of Engineering and Built Environment, The University of Newcastle, Australia
[b] Faculty of Bridge and Road Engineering, University of Science and Technology, The University of Danang, Viet Nam
[c] Chief Technical Principal of Geotechnics, SMEC, Australia

Received 20 June 2016; received in revised form 15 March 2017; accepted 23 April 2017
Available online 20 June 2017

Abstract

The soil-cement column is a ground improvement technique formed by the deep mixing method. In coastal areas, the soil-cement columns can deteriorate due to the attack of sulfate present in sea water. After long periods of exposure, the strength of these columns may decrease significantly, ultimately resulting in failure in the worst case scenario. In this study, needle penetration tests, uniaxial compression tests and a thermogravimetric analysis were applied to determine the extent of the deterioration of soil-cement columns exposed to synthetic sea water. An analysis model was developed and calibrated using the experimental data to predict the change in the total strength of the soil-cement columns as a function of time. The results show that the deterioration rate increases when the diameter of the samples decreases. The model proposed has potential to be used to design more durable soil-cement columns in coastal environments.

Keywords: Soil-cement column; Needle penetration test; Thermogravimetric analysis; Sulfate concentrations; Deterioration depth; Total strength change; Strength prediction model

1. Introduction

The deep mixing method (DMM) is a soil stabilizing treatment technique which is commonly applied in many countries and is also used in the production of stabilized soil-cement columns. In this technique, in-situ soil is mixed with cement to create a high stiffness soil-cement column (Alfaro et al., 1994; Broms and Boman, 1979). This method has many advantages: it is technologically simple, low cost, allows for fast construction, and the end product has low permeability (Bruce, 2000; Chen et al., 2013; Dehghanbanadaki et al., 2013; Kitazume and Terashi, 2013).

Among the many factors that affect the properties of the soil-cement columns, the binder type, soil characteristics, and mixing and curing conditions are the most important (Kitazume and Terashi, 2013). It is well-documented that in sea water environments or marine deposited soils, sulfate can attack the columns causing a deterioration in strength (Rajasekaran, 2005). Loss of column strength occurs as sulfate dissolves the pozzolanic minerals developed during the concretion of the stabilized columns, producing ettringite and magnesium hydroxide (Mather, 1964; Rajasekaran and Narasimha Rao, 2005). Consequently, the strength of the soil–cement column is significantly reduced and the surface of the column can crack (Mather, 1964; Neville, 1995; Rajasekaran, 2005).

In sea water environments, the strength at the outer surface of the column can decrease due to sulfate attack (Hayashi et al., 2002; Ikegami et al., 2005; Kitazume

Peer review under responsibility of The Japanese Geotechnical Society.
* Corresponding author at: Faculty of Engineering and Built Environment, The University of Newcastle, Australia.
E-mail addresses: vanngoc.pham@uon.edu.au (V.N. Pham), brett.turner@newcastle.edu.au (B. Turner), jinsong.huang@newcastle.edu.au (J. Huang), richard.kelly@smec.com (R. Kelly).

http://dx.doi.org/10.1016/j.sandf.2017.04.005
0038-0806/

Nomenclature

C	cement ratio
CH	porlandite – $Ca(OH)_2$
D	diameter
F	resistance force
F_s	safety factor
$L_{eq.}$	equivalent deterioration depth
ML	mass loss
MM	molar mass
NPR	needle penetration resistance
P	bearing capacity
$[P]$	required bearing capacity
P_a	allowable bearing capacity
P_{nd}	bearing capacity of non-deteriorated soil-cement column
P_d	bearing capacity of deteriorated soil-cement column
R^2	correlation coefficient
R_P	loss ratio
SW	sea water
TGA	thermogravimetric analysis
TGA-DSC	thermogravimetric analysis with differential scanning calorimetry
UCS	unconfined compressive strength
α	coefficient of effective width
β	reliability coefficient of overlapping
γ	correction factor for strength variability
d	diameter of non-deteriorated portion
h	height
q_u	unconfined compressive strength
$[q_u]$	required unconfined compressive strength
$[q_u^{28}]$	required unconfined compressive strength at 28 days
t	time
r	deterioration depth

et al., 2002; Terashi et al., 1980). Fig. 1 illustrates the long-term strength development of a soil-cement column exposed to sea water. For the unaffected core portion, while the strength gain proceeds in accordance with concrete theory, the column surface deteriorates due to attack by sea water. Consequently, the significantly reduced strength at the outer surface of the column with time results in an overall reduction in total strength and, therefore, a reduction in the bearing capacity of the column. This suggests that it is necessary to determine when a given soil-cement column will lose its bearing capacity.

There have been very few publications on the long-term strength of stabilized soils exposed to sea water. It has been concluded that the strength at the surface of columns exposed to sea water decreases significantly and that this can be attributed largely to calcium leaching (Hayashi et al., 2002; Ikegami et al., 2005; Kitazume et al., 2002; Terashi et al., 1980). In addition, Nishida et al. (2002) observed strength changes in cement treated soil in Hokkaido, Japan, after 17 years and developed a calcium leaching model to predict the strength of these columns in which the deterioration process was proportional to the square root of time.

Recently, Cui et al. (2014) provided a method to predict the deterioration process of cement treated soil in a saltwater estuarine region. The soils were treated with high amounts of cement and exposed to a low sulfate concentration. They reported only small changes in the strength of the soil-cement columns.

The purpose of this research is to measure the long-term strength of laboratory prepared soil-cement samples exposed to sea water using a soil obtained from the coast of Newcastle, New South Wales, Australia. Needle penetration tests, uniaxial compression tests and a thermogravimetric analysis were carried out to determine the strength gain at the core portion and the extent of strength deterioration at the outer surface of the soil-cement samples over a 12-month period. The experimental data was then used to develop a model to determine the long-term strength changes as a function of time. This model can be used to evaluate the durability of the soil-cement columns contacted directly with sea water.

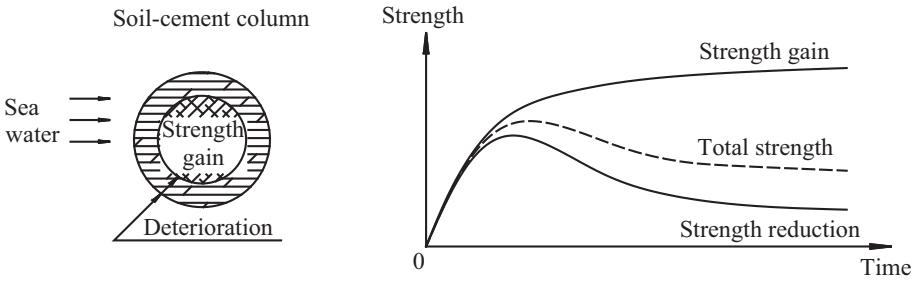

Fig. 1. Long-term strength of the soil-cement column.

2. Materials and methods

2.1. Soil-cement samples preparation

The soil used in the research was collected from the Rail Flyover Modification project, Newcastle, New South Wales, Australia. Its characteristics are shown in Table 1. A dry mixing method (i.e. no liquid added) was applied to stabilize the soil with a cement content of 120 kg/m^3 to achieve the required unconfined compressive strength of 250 kPa at 28 days. A mold made from PVC pipe with a diameter of 53.2 mm and a height of 106.4 mm was used to prepare specimens in accordance with the Japanese standard (JGS, 2005). The diameter, weight and height of samples were then measured to determine sample density. Only samples with a density of at least 1.9 ± 0.01 g/cm^3 were used for further experiments.

Sixty-five specimens were divided into 4 groups, namely G0, G1, G2 and G3 as shown in Table 2. All of the specimens were cured in a fog room with a constant humidity of 95%. After 28 days of curing, when the specimens reached the standard strength, the soil-cement samples were taken out of the cylinder molds. At that time, uniaxial compression tests were conducted to measure the initial strength of the samples in group G0. The specimens in group G1, which were sealed in a container and cured under standard conditions at 20 degrees in Celsius (°C) and 95% relative humidity, were used as control samples. Groups G2 and G3 were submerged in synthetic (100%) sea water (SW) and synthetic (200%) sea water made up to twice the concentration of that used for 100% SW. These specimens were tested at the time of 58 days, 118 days, 208 days and 388 days.

Table 1
Soil characteristic.

Properties	Value
Calcium (mg/kg)	4351.02
Magnesium (mg/kg)	2531.91
Potassium (mg/kg)	1561.31
Sodium (mg/kg)	1521.66
Phosphorus (mg/kg)	183.69
Sulfate (mg/kg)	785.61
Silicon (mg/kg)	367.0
Manganese (mg/kg)	107
Water content (%)	37.7
Liquid limit (%)	25
Plastic limit (%)	19
Density (g/cm^3)	1.68

*Note: Soil classification: clayey-sand.

Table 2
Experimental test matrix.

Group	G0	G1	G2	G3
Exposure condition	–	Control	100% SW	200% SW
Number of specimens	5	20	20	20
Uniaxial compression test	x	x	x	x
Needle penetration resistance	–	x	x	x
Thermogravimetric analysis	–	x	–	–

2.2. Uniaxial compression test

The uniaxial compression test was conducted to measure the unconfined compressive strength of all stabilized soil samples using standard D2166-06. The compressive rate of 1 mm/min was applied for these tests giving the axial strain rate on the specimen of 0.625%/min (in the range of 0.5–2%/min as a recommendation of the standard).

2.3. Needle penetration resistance (NPR) test

While the needle penetration test is not a standardized test, it is used in concrete and soft rock tests (Klimesch and Ray, 1997; Ngan-Tillard et al., 2011; Ulusay and Erguler, 2012). Japanese researchers developed the needle penetration system to indirectly determine the strength distribution of stabilized soil (Hayashi et al., 2002; Kitazume et al., 2002; Takashi et al., 1999).

A needle penetration test system was designed and constructed in house based on the work of Kitazume et al. (2002). A needle with a diameter of 0.75 mm and a length of 15 mm was used to penetrate the samples. To measure the needle penetration resistance force, a load-cell (0.5 kN) was used in conjunction with the compression machine. During the test, a penetration speed of 1 mm/min was applied and the resistance force was recorded continuously (Kitazume et al., 2002). The relationship between the UCS and NPR allows the radial strength change of the stabilized soil (deterioration level) to be assessed.

2.4. Thermogravimetric analysis

Thermogravimetric Analysis with Differential Scanning Calorimetry (TGA-DSC) is a technique used to measure the thermodynamic and mass change of a material as a function of temperature and/or time. In terms of soil-cement mixing, TGA-DSC can be used to measure the weight loss to determine the amount of calcium consumption during hydration and pozzolanic reactions. Therefore, if the TGA results of the soil-cement sample show a small amount of calcium consumption, it reflects a high level of deterioration and large amount of calcium leaching (Horpibulsuk et al., 2013; Matschei, 2007).

The tests were conducted by heating the samples from 25 to 1000 °C at a rate of 10 °C/min (Mertens et al., 2009). To prevent sample oxidation, nitrogen gas was injected into the system at 60 ml/min (Mertens et al., 2009). The mass losses in the range of 400–500 °C and 600–800 °C are the free portlandite and carbon-dioxide (CO_2) due to portlandite dehydration and carbonate decomposition in the samples, respectively (Damidot et al., 2011; Lawrence et al., 2006; Silva et al., 2014).

These values can be measured from TGA results and through the application of Eqs. (1) and (2) (Silva et al.,

2014). In the research, the amount of calcium consumption at the positions of 2 mm, 5 mm and 10 mm depth of the soil-cement samples were measured through Eq. (3) (Silva et al., 2014).

$$CH_{free} = (ML_{CH(400–500\ ^\circ C)} \times MM_{CH})/MM_{H_2O} \quad (1)$$

$$CH_{carbonation} = (ML_{CO_2(600–800\ ^\circ C)} \times MM_{CaCO_3})/MM_{CO_2} \quad (2)$$

$$CH_{cal\ consumption} = CH_{cal^0} - (CH_{free} + CH_{carbonation}) \quad (3)$$

where CH_{free} is the free portlandite ($Ca(OH)_2$) content; $ML_{CH(400–500\ ^\circ C)}$ is the mass loss between 400 and 500 °C corresponding to portlandite dehydration; MM_{H_2O} is the molar mass of H_2O, (18 g/mol); MM_{CH} is the molar mass of the portlandite, (74.09 g/mol); $CH_{carbonation}$ is the calcium consumed in the carbonation reaction; $ML_{CO_2(600–800\ ^\circ C)}$ is the mass loss between 600 and 800 °C corresponding to carbonate decomposition; MM_{CaCO_3} is the molar mass of $CaCO_3$, (100.08 g/mol); MM_{CO_2} is the molar mass of CO_2, (48 g/mol); CH_{cal^0} is the initial calcium content in cement, $CH_{cal^0} = 65\%$ (as per manufactures specifications of GP cement); $CH_{cal\ consumption}$ is the calcium consumption in hydration and pozzolanic reactions.

3. Results

3.1. Unconfined compressive strength

Research has shown that the unconfined compressive strength (UCS) of the soil-cement columns under non-saline conditions is a function of the logarithm of time (Hayashi et al., 2002; Kitazume et al., 2002; Saitoh, 1988). Consequently, the long-term compressive strength gain of the non-deteriorated soil-cement columns can be expressed in the following way:

$$q_u = A + B\ln(t) \quad (4)$$

where q_u is the strength of the soil-cement column (kN/m^2); t is the age of the soil-cement column (day); A and B are constants.

The results of the uniaxial compression tests of the control samples which cured in air at 20 °C and 95% humidity are plotted in Fig. 2. It can be seen that the strength of the soil-cement samples has a linear relationship with logarithm of time as supported by Hayashi et al. (2002). Therefore, the strength gain of the non-deteriorated soil-cement samples (control samples) is expressed as

$$q_u = 290.59 + 438.55\ln t \quad (R^2 = 0.98) \quad (5)$$

where R^2 is correlation coefficient, which implies the fitting precision. Eq. (5) can be used to predict the long-term strength of the (control) soil-cement columns.

3.2. Needle resistance calibration

The needle penetration resistance (NPR) forces at the depths of 2 mm, 5 mm and 10 mm, and the unconfined compressive strength (UCS) results of soil-cement samples

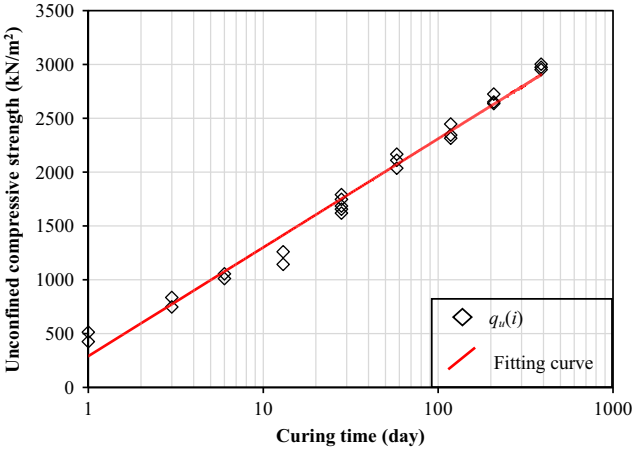

Fig. 2. Strength gain of the soil-cement column ($C = 120$ kg/m^3).

are plotted in Fig. 3. It is clear that the NPR has a linear relationship with the UCS. Eqs. (6)–(8) are fitted relationships between NPR and UCS at different depths.

$$q_{u-2mm} = 138.55 \times F_{2mm} \quad (6)$$

$$q_{u-5mm} = 50.183 \times F_{5mm} \quad (7)$$

$$q_{u-10mm} = 32.658 \times F_{10mm} \quad (8)$$

where $q_{u\text{-}2mm}$, $q_{u\text{-}5mm}$, and $q_{u\text{-}10mm}$ are the strengths (kN/m^2) at the penetration depths of 2 mm, 5 mm and 10 mm; F_{2mm}, F_{5mm}, and F_{10mm} are the needle penetration resistance forces (N) at the penetration depths of 2 mm, 5 mm and 10 mm, respectively.

3.3. Needle penetration resistance

The needle penetration resistance forces of the control, 100% SW and 200% SW samples at four different times are plotted in Figs. 4–7. The effect of the sulfate attack at the surface portion of the deteriorated samples is smaller than the control samples, according to the needle penetration resistance forces. Therefore, the depth of deterioration (r) of the soil-cement samples can then be determined by the depth at which the deterioration curves meet the con-

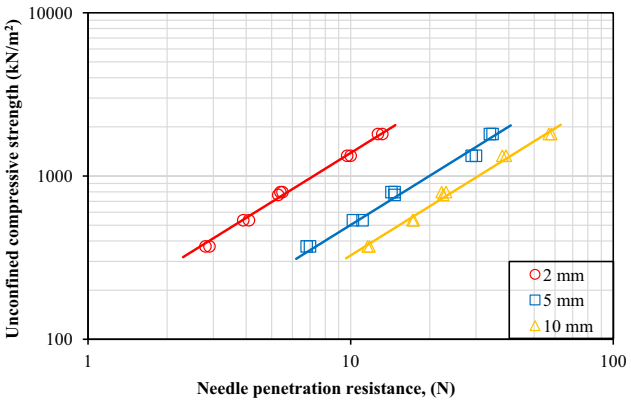

Fig. 3. The relationship between the UCS and the NPR.

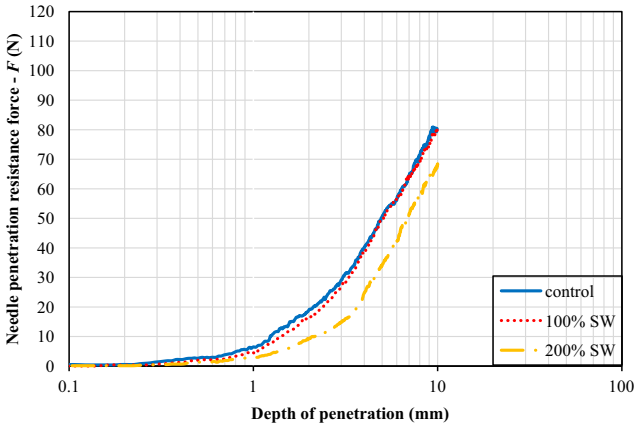

Fig. 4. Needle penetration resistance at 58 days.

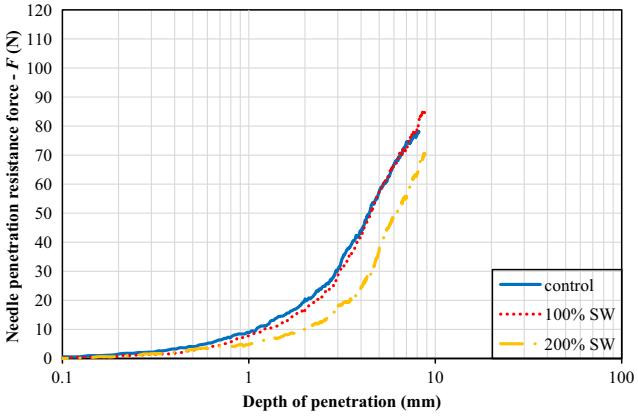

Fig. 5. Needle penetration resistance at 118 days.

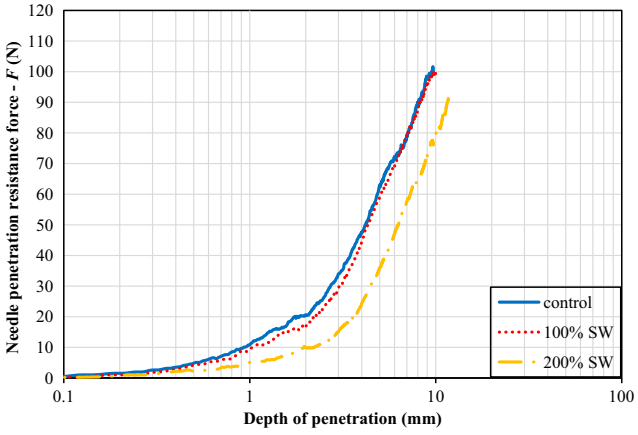

Fig. 6. Needle penetration resistance at 208 days.

trol curves. It can be seen from these figures that the deterioration curves of the samples exposed to 100% SW meet the control curves at the depths of 3.81 mm, 4.78 mm, 6.34 mm and 8.51 mm at the time of 58 days, 118 days, 208 days and 388 days, respectively (as shown in Table 3). These depths are deemed to be the deterioration depths.

The deterioration occurs more quickly than in the samples exposed to 200% SW than those exposed to 100% SW.

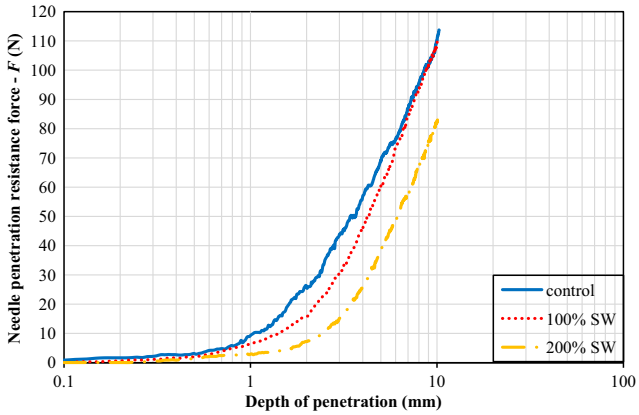

Fig. 7. Needle penetration resistance at 388 days.

Table 3
The depths of deterioration in case of 100% SW.

Time (day)	NPR results (mm)	TGA results (mm)
58	3.81	3.88
118	4.78	4.61
208	6.34	6.59
388	8.51	8.34

The deterioration curves of 200% SW samples shown in Figs. 4–7 are obviously below the control curves. Therefore, it is necessary to conduct more experiments to determine the depth of deterioration of the soil-cement samples exposed to 200% SW.

3.4. TGA results

TGA results at depths of 2 mm, 5 mm and 10 mm of the soil-cement samples are shown in Figs. 8–11. The depth of deterioration can be measured from the TGA results calculating the calcium consumption according to Eqs. (1)–(3). The calcium consumption of the control samples fluctuates slightly from 57% to 58%. However, because the calcium consumption at the outer surface of the samples exposed to sea water is much lower than inside, it can be concluded that a large amount of calcium is leached at these locations. The calcium leached from the samples as the effects of sulfate could be measured by TGA analysis.

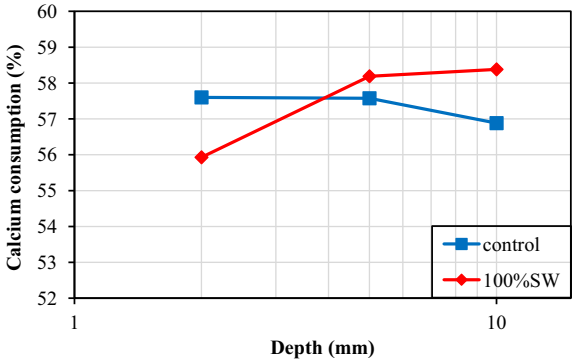

Fig. 8. TGA result at 58 days.

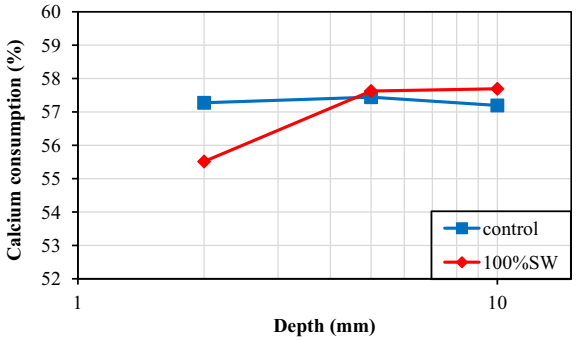

Fig. 9. TGA result at 118 days.

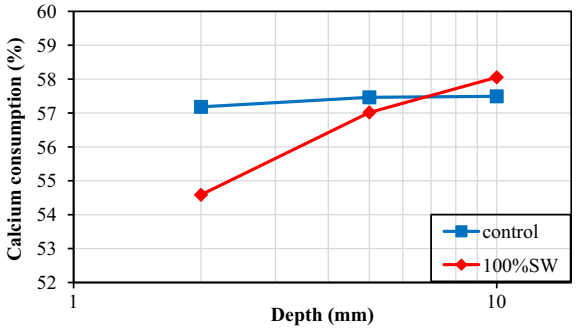

Fig. 10. TGA result at 208 days.

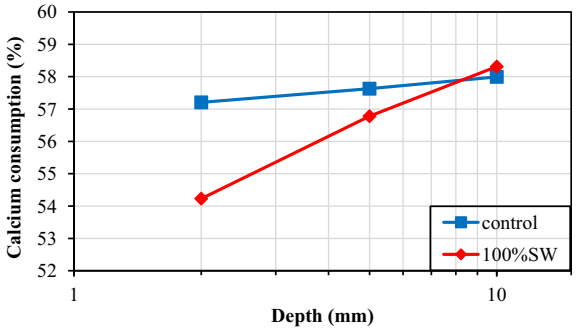

Fig. 11. TGA result at 388 days.

In terms of the deterioration depths of the samples exposed to 100% SW, Figs. 8–11 show that the TGA curves of these samples meet the control curves at the depths of 3.88 mm, 4.61 mm, 6.59 mm and 8.34 mm at the time of 58 days, 118 days, 208 days and 388 days, respectively. These results are compared with the results from needle penetration tests in Table 3. It can be seen from Table 3 that the depths of deterioration of the soil-cement samples exposed to 100% SW obtained from the TGA analysis are similar with the results of the needle penetration tests.

4. Prediction of the depth of deterioration

The deterioration depth of the soil-cement samples exposed to 100% SW was determined by the needle penetration test and TGA analysis. The results obtained from these tests shown the same trend of deterioration. By combining these results, a more reliable prediction model of deterioration depth can be developed.

According to Ikegami et al. (2005) and Nishida et al. (2002), the deterioration progress is approximately linear with the logarithmic time, and the deterioration depth is a function of the square root of time. The deterioration depth of the soil-cement columns is therefore determined as

$$\frac{\log r - \log r_0}{\log t - \log t_0} = \frac{1}{2} \tag{9}$$

where r is the deterioration depth (mm) at t; r_0 is the deterioration depth at t_0; and t is the time (day) from t_0.

The deterioration depths of the soil-cement samples exposed to SW observed from needle penetration tests are plotted in Fig. 12. It is clear that the trend of deterioration depth is similar to that of Ikegami et al. (2005) and Nishida et al. (2002), and the depth of the deterioration of soil-cement samples can be expressed as

$$r = 0.45\sqrt{t} \quad (R^2 = 1) \tag{10}$$

However, because the soil-cement samples were immersed in sea water after 28 days curing in air in this study, deterioration does not occur at $t = 28$ days ($r = 0$). Therefore, Eq. (10) is applied for $t > 28$ days only (i.e. only after exposure to sea water).

5. Predicting the long-term strength of the soil-cement columns

5.1. Strength prediction model

In marine environments, there are two process in the change in strength that occur in the soil-cement columns: the strength gain at the core portion of the columns, and the strength deterioration at outer boundary as shown in Fig. 13. Hence, the total bearing capacity of the soil-cement column can be determined as

$$P = q_u(r,t)\frac{\pi d^2}{4} + \int_0^r 0.5\pi(D-x)q_u(x,t)dx \tag{11}$$

where P is the total bearing capacity of the soil-cement column (kN); $q_u(r,t)$ is strength at the non-deteriorated por-

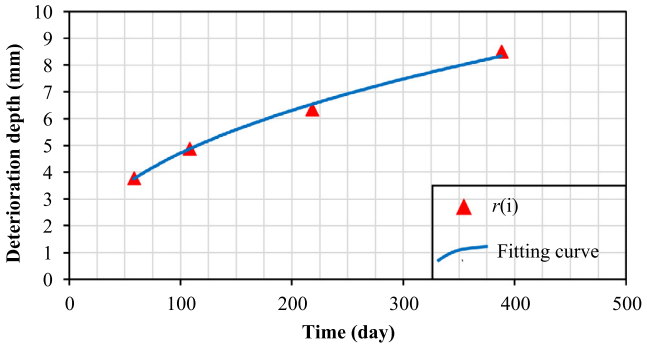

Fig. 12. Deterioration depth by the time in case of 100% SW.

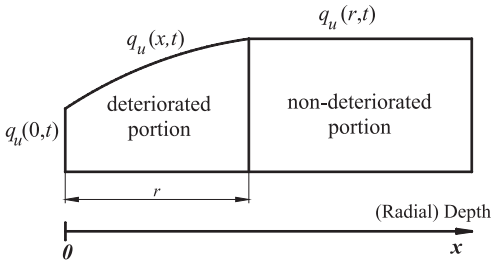

Fig. 13. Strength distribution in the soil-cement column.

tion of the column; $q_u(x,t)$ is the strength of the deteriorated portion; D is the diameter of the column (mm); t is the age of the column (day); and d is the diameter of non-deteriorated portion, $d = D - 2r$.

Fig. 13 shows that $q_u(x,t)$ depends on three main parameters $q_u(r,t)$, r and $q_u(0,t)$. For $q_u(r,t)$, the strength gain of the non-deteriorated part of the column depends on composition and time. It is equal to the strength of the soil-cement column cured under the control condition as shown in Eq. (5). The deterioration depth, r, depends on the effects of sea water, composition and time. For the soil-cement column exposed to 100% SW, the deterioration depth can be determined by Eq. (10).

The strength at the surface of the samples exposed to sea water, $q_u(0,t)$, also depends on the effects of sea water, composition and time. Because the head of the needle used in this study was tiny and sharp, $q_u(0,t)$ could not be measured by the needle penetration test. Therefore, the strength at 2 mm, which were converted from the measured NPR using Eq. (6), was used as $q_u(0,t)$. In addition, a ratio of strength at the surface of the deteriorated samples to the control samples, $q_u(0,t)/q_u(r,t)$, was used to determine the effects of sea water on the outer position. The strength ratio of the soil-cement samples exposed to 100% SW obtained from Fig. 14 is expressed as

$$\frac{q_u(0,t)}{q_u(r,t)} = 1.522 - 0.152\ln t \tag{12}$$

Eq. (5) is substituted into Eq. (12) to obtain the strength at the surface of the soil-cement columns:

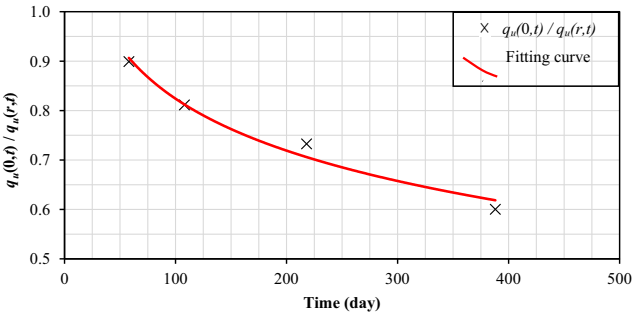

Fig. 14. Strength ratio at the surface of the samples.

$$q_u(0,t) = (1.522 - 0.152\ln t) \times (290.59 + 439.55\ln t) \quad (R^2 = 0.98) \tag{13}$$

Solving Eq. (13) at $q_u(0,t) = 0$ gives $t = 22318$ days.

Fig. 15 and Table 4 show the ratios of the strength at the deteriorated positions of the samples exposed to 100% SW to the strength of the control samples, $q_u(x,t)/q_u(r,t)$. It can be seen that strength change at the deteriorated portion can be expressed as a function of the logarithm of depth ($\ln x$). Moreover, the boundary conditions of $q_u(x,t)$ obtained from Fig. 13 include

For $x = 0$,

$$q_u(x,t) = q_u(0,t) \tag{14}$$

For $x = r$,

$$q_u(x,t) = q_u(r,t) \tag{15}$$

Then, the strength at the deteriorated positions of the samples is expressed as

$$q_u(x,t) = \frac{q_u(r,t) - q_u(0,t)}{\ln r}\ln x + q_u(0,t) \tag{16}$$

The bearing capacity of the soil-cement column exposed to 100% SW can be calculated by the following: (see Fig. 16)

If $t < 22318$ *days*,

$$P = q_u(r,t)\frac{\pi d^2}{4} + \pi\frac{r(D-r)[q_u(r,t)\ln r - q_u(r,t) + q_u(0,t)]}{\ln r} \tag{17}$$

If $t \geqslant 22318$ *days*,

$$P = q_u(r,t)\frac{\pi d^2}{4} + \pi\frac{r(D-r)[q_u(r,t)\ln r - q_u(r,t) - |q_u(0,t)|]}{\ln r} - \pi\frac{L(t)(D-r)[q_u(r,t) + |q_u(0,t)|\ln L(t) + q_u(r,t)\ln r - q_u(r,t) - |q_u(0,t)|]}{\ln r} \tag{18}$$

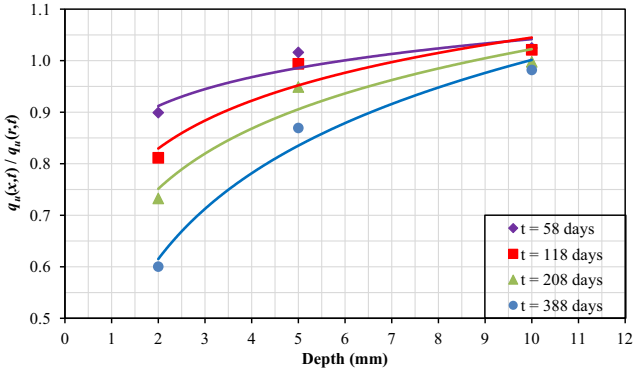

Fig. 15. Strength distribution at the deteriorated portion of the samples.

Table 4
Strength change trend at the deteriorated portion.

Time (day)	$q_u(x,t)$	R^2
58	$q_u(x,58) = 0.0806\ln(x) + 0.8563$	0.86
118	$q_u(x,118) = 0.1338\ln(x) + 0.7367$	0.90
208	$q_u(x,208) = 0.1685\ln(x) + 0.6346$	0.92
388	$q_u(x,388) = 0.2401\ln(x) + 0.4486$	0.98

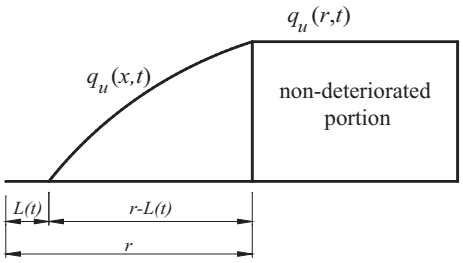

Fig. 16. Strength distribution when $t > 228318$ days.

where $|q_u(0,t)|$ is the absolute value of $q_u(0,t)$ when $t \geqslant 22318 days$; $L(t)$ is the depth when $q_u(x,t) = 0$. $L(t)$ can be calculated by:

$$L(t) = e^{\frac{|q_u(0,t)| \cdot \ln r}{q_u(r,t)+|q_u(0,t)|}} \quad (19)$$

5.2. Model calibration

Table 5 and Fig. 17 demonstrate the total bearing capacity of the soil-cement columns with the diameter of 54 mm calculated by Eqs. (17) and (18) in comparison with experimental results of the control samples and the samples exposed to 100% SW. It is clear that the results calculated by the analysis model are very close to the experimental data. Therefore, this analysis model can be used to predict the strength change of the soil-cement columns exposed to sea water.

5.3. Model application

Fig. 18 shows the predicted bearing capacity of the columns exposed to sea water with various column diameters $D = 0.3$ m, 0.5 m and 0.7 m. It can be seen from Fig. 18 that the deterioration rate increases as the size of the column decreases.

To determine the level of deterioration, a loss ratio was calculated by dividing the reduction of bearing capacity of deteriorated columns to the total bearing capacity of the non-deteriorated columns.

$$R_p = \frac{P_{nd} - P_d}{P_{nd}} \quad (20)$$

where R_P is the loss ratio; P_{nd} is the bearing capacity of the non-deteriorated soil-cement column; and P_d is the bearing capacity of the deteriorated soil-cement column.

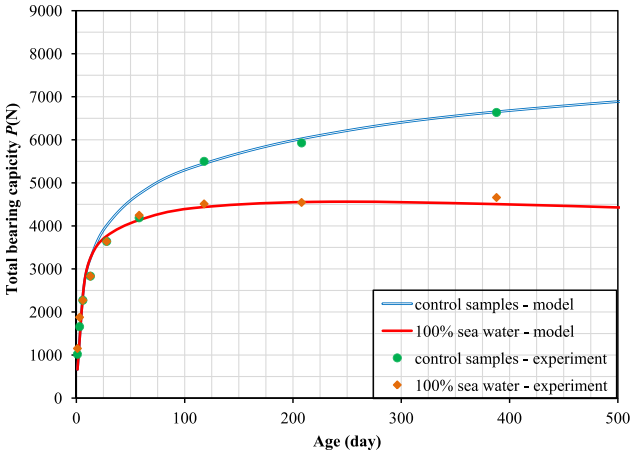

Fig. 17. Total bearing capacity of soil-cement columns ($D = 54$ mm).

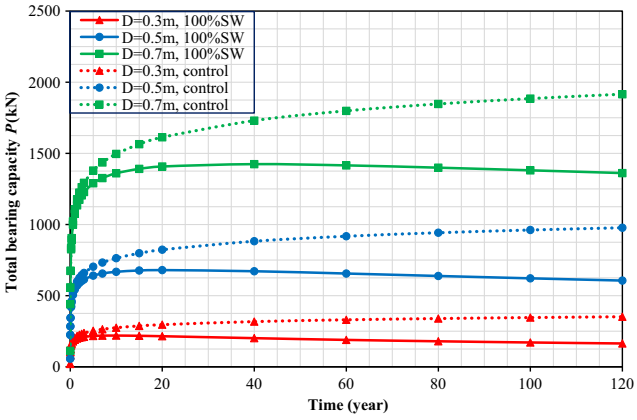

Fig. 18. Predicted bearing capacity of soil-cement column exposed to 100% SW.

Fig. 19 shows the loss ratio of deteriorated columns with the diameters of $D = 0.3$ m, 0.5 m and 0.7 m. For the $D = 0.7$ m column, about 25% of the bearing capacity is lost after 100 years while the column with $D = 0.3$ m shows double the deterioration rate for the same period. That is, the smaller column has a faster deterioration rate.

To evaluate the durability of the soil-cement columns, it is necessary to determine a required bearing capacity and an allowable bearing capacity of the soil-cement columns. According Kitazume and Terashi (2013), the required bearing capacity can be calculated as follows:

Table 5
The comparison between prediction model and experimental result.

Time (day)	r (mm)	q_u (kN/m^2)	P_1 (N)	P_2 (N)	Prediction model		Experimental result	
					P (N) (100% SW)	P (N) (control samples)	P (N) (100% SW)	P (N) (control samples)
58	3.43	2071.09	3615.56	520.28	4135.84	4743.26	4247.23	4188.31
108	4.68	2343.70	3669.24	744.76	4414.00	5367.60	4510.97	5499.25
218	6.64	2651.69	3451.84	1105.41	4557.25	6072.96	4544.29	5927.34
388	8.86	2904.49	3001.26	1504.04	4505.30	6651.93	4659.60	6635.57

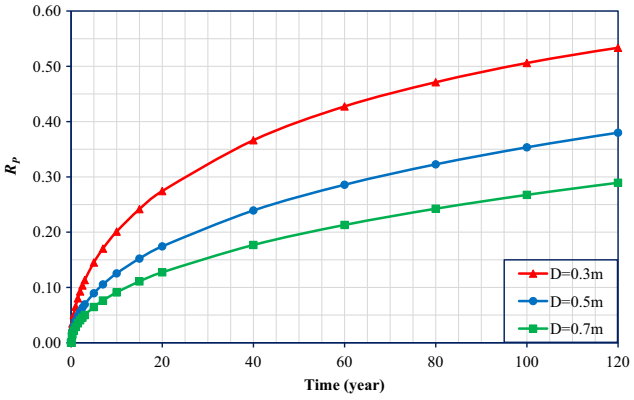

Fig. 19. The loss ratio of bearing capacity of soil-cement columns.

$$[P] = 2.5\frac{\pi}{4}D^2[q_u^{28}] \tag{21}$$

where $[q_u^{28}]$ is the required unconfined compressive strength at 28 days, $[q_u^{28}] = 250$ kPa.

The allowable bearing capacity can be calculated by

$$P_a = \frac{1}{F_s}\alpha\beta\gamma P \tag{22}$$

where α is coefficient of effective width of the column (0.8–0.9); β is reliability coefficient of overlapping (0.8–0.9); γ is correction factor for strength variability, $\gamma = 0.55$; F_s is safety factor, $F_s = 2$; and P is total bearing capacity of the column (kN).

In Fig. 20, the ratios between the allowable bearing capacity and the required bearing capacity ($P_a/[P]$) show that within 45 years, the allowable bearing capacity of the soil-cement columns is higher than the required bearing capacity ($P_a > [P]$) in the case of $D = 0.3$ m. Nevertheless, after that period the structure can collapse because the bearing capacity of the column is lower than the required bearing capacity ($P_a < [P]$). Therefore, it is of utmost importance to take size into account when designing soil-cement columns in coastal areas.

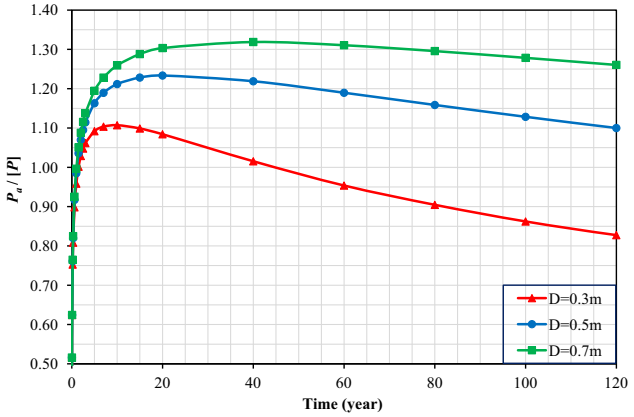

Fig. 20. The durability of the soil-cement column.

6. Conclusions

In this study, experiments on the strength change of the soil-cement column were conducted by the uniaxial compression test, needle penetration resistance and TGA analysis. In addition, the strength prediction model was developed to predict the total strength change of the soil-cement columns constructed in sea water. The results of this study can be summarized as follows:

1. The needle penetration resistance test is a suitable method to determine the depth of deterioration in soil-cement columns.
2. At high sulfate concentrations, the deterioration process in the soil-cement column occurs at a faster rate, which results in deeper penetration.
3. TGA analysis can be used to determine the amount calcium consumption in both hydration and the pozzolanic reaction in the soil-cement column. The free portlandite ($Ca(OH)_2$) mass loss between 400 and 500 °C can be used to calibrate the soil-cement column durability model.
4. The proposed model can be used to predict the change in strength of the non-deteriorated as well as the deteriorated portion of the soil-cement columns exposed to synthetic sea water.
5. The deterioration of smaller diameter soil-cement columns displays a higher rate of strength loss. For example, soil-cement columns with a diameter of 0.3 m exposed to sea water may collapse ($P_a < [P]$) after 45 years. As such, the size of the columns should be carefully considered in the design of soil-cement columns in coastal areas.

Acknowledgement

This research was partially supported by Keller Ground Engineering Pty Ltd., who provided the soil samples collected from the Newcastle Rail Flyover Modification project, Australia. We are also thankful to Lachlan Bates for his co-operation and support of the research.

References

Alfaro, M., Balasubramaniam, A., Bergado, D., Chai, J., 1994. Improvement Techniques of Soft Ground in Subsiding and Lowland Environment. CRC Press.

Broms, B.B., Boman, P., 1979. Lime columns-a new foundation method. J. Geotech. Geoenviron. Eng., 105(ASCE 14543).

Bruce, D.A., 2000. An introduction to the deep soil mixing methods as used in geotechnical applications.

Chen, J.J., Zhang, L., Zhang, J.F., Zhu, Y.F., Wang, J.H., 2013. Field tests, modification, and application of deep soil mixing method in soft clay. J. Geotech. Geoenviron. Eng., 24–34

Cui, X., Zhang, N., Li, S., Zhang, J., Tang, W., 2014. Deterioration of soil-cement piles in a saltwater region and its influence on the settlement of composite foundations. J. Perform. Constructed Facilities, 04014195.

Damidot, D., Lothenbach, B., Herfort, D., Glasser, F., 2011. Thermodynamics and cement science. Cem. Concr. Res. 41 (7), 679–695.
Dehghanbanadaki, A., Ahmad, K., Ali, N., Khari, M., Alimohammadi, P., Latifi, N., 2013. Stabilization of soft soils with deep mixed soil columns. EJGE 18, 295–306.
Hayashi, H., Nishikawa, J.i., Ohishi, K., Terashi, M., 2002. Field observation of long-term strength of cement treated soil. Geotech. Spec. Publ. 1, 598–609.
Horpibulsuk, S., Phetchuay, C., Chinkulkijniwat, A., Cholaphatsorn, A., 2013. Strength development in silty clay stabilized with calcium carbide residue and fly ash. Soils Found. 53 (4), 477–486.
Ikegami, M., Ichiba, T., Ohishi, K., Terashi, M., 2005. Long-term properties of cement treated soil 20 years after construction. Proc. Int. Conf. Soil Mech. Geotech. Eng.
JGS, 2005. Japanese Geotechnical Society Standard "Practice for making and curing stabilized soil specimens without compaction" (JGS 0821-2000). In: International Conference on Deep Mixing Best Practice and Recent Advances.
Kitazume, M., Nakamura, T., Terashi, M., Ohishi, K., 2002. Laboratory tests on long-term strength of cement treated soil. Geotech. Spec. Publ. 1, 586–597.
Kitazume, M., Terashi, M., 2013. The Deep Mixing Method. Taylor and Francis, London.
Klimesch, D.S., Ray, A., 1997. The use of DTA/TGA to study the effects of ground quartz with different surface areas in autoclaved cement: quartz pastes. Use of the semi-isothermal thermogravimetric technique. Thermochim. Acta 306 (1), 159–165.
Lawrence, R., Mays, T., Walker, P., D'ayala, D., 2006. Determination of carbonation profiles in non-hydraulic lime mortars using thermogravimetric analysis. Thermochim. Acta 444 (2), 179–189.
Mather, B., 1964. Effects of Sea Water on Concrete. U.S. Army Corps of Engineers.
Matschei, T., 2007. Thermodynamics of Cement Hydration. Aberdeen University.
Mertens, G., Snellings, R., Van Balen, K., Bicer-Simsir, B., Verlooy, P., Elsen, J., 2009. Pozzolanic reactions of common natural zeolites with lime and parameters affecting their reactivity. Cem. Concr. Res. 39 (3), 233–240.
Neville, A.M., 1995. Properties of Concrete. Pearson, London.
Ngan-Tillard, D., Verwaal, W., Mulder, A., Engin, H., Ulusay, R., 2011. Application of the needle penetration test to a calcarenite, Maastricht, the Netherlands. Eng. Geol. 123 (3), 214–224.
Nishida, T., Terashi, M., Otsuki, N., Ohishi, K., 2002. Prediction method for Ca leaching and related property change of cement treated soil. Grouting and Ground Treatment.
Rajasekaran, G., 2005. Sulfate attack and ettringite formation in the lime and cement stabilized marine clays. Ocean Eng. 32 (8), 1133–1159.
Rajasekaran, G., Narasimha Rao, S., 2005. Sulfate attack in lime-treated marine clay. Mar. Georesour. Geotechnol. 23 (1–2), 93–116.
Saitoh, S., 1988. Experimental study of engineering properties of cement improved ground by the deep mixing method. PhD. Thesis, Nihon University.
Silva, A.S., Gameiro, A., Grilo, J., Veiga, R., Velosa, A., 2014. Long-term behavior of lime–metakaolin pastes at ambient temperature and humid curing condition. Appl. Clay Sci. 88, 49–55.
Takashi, M., Ichiro, I., Hirofusa, I., 1999. Study on evaluating deterioration of concrete structure using needle penetration test. J. Mater., Concr. Struct. Pavements 620, 245–255.
Terashi, M., Tanaka, H., Mitsumoto, T., Niidome, Y., Honma, S., 1980. Fundamental properties of lime and cement treated soils (2nd report). Report Port Harbour Res. Inst. 19 (1), 33–62.
Ulusay, R., Erguler, Z., 2012. Needle penetration test: evaluation of its performance and possible uses in predicting strength of weak and soft rocks. Eng. Geol. 149, 47–56.